

Quantitative Susceptibility Mapping for Characterization of Intraplaque Hemorrhage and Calcification in Carotid Atherosclerotic Disease

Chaoyue Wang, Msc^{1,2,3}, Yue Zhang¹, Jingwen Du¹, István N. Huszár, MD^{2,3}, Saifeng Liu, PhD⁴,
Yongsheng Chen, PhD^{4,5}, Sagar Buch, PhD⁶, Fang Wu, MD¹, Yuehong Liu¹, Mark Jenkinson,
PhD^{2,3}, Charlie Chia-Tsong Hsu, PhD⁷, Zhaoyang Fan, PhD⁸, E. Mark Haacke, PhD^{4,5} Qi Yang,
MD, PhD^{1,8}.

¹Department of Radiology, Xuanwu Hospital, Capital Medical University, Beijing, China, 100053;

²Nuffield Department of Clinical Neurosciences, University of Oxford, Oxford, UK, OX3 9DU

³Wellcome Centre for Integrative Neuroimaging, FMRIB, Nuffield Department of Clinical Neurosciences, University of Oxford, Oxford, UK, OX3 9DU

⁴Magnetic Resonance Imaging Institute for Biomedical Research, Bingham Farms, MI, USA, 48025

⁵Department of Radiology, Wayne State University, Detroit, MI, USA, 48201;

⁶Center for Functional and Metabolic Mapping, Robarts' research institute, Western University, London, ON, Canada, N6G 2V4;

⁷Gold Coast University Hospital, Southport, Queensland, Australia, 4215;

⁸Biomedical Imaging Research Institute, Cedars Sinai Medical Center, Los Angeles, CA, USA, 90048;

Corresponding Author: Qi Yang, MD, PhD, Department of Radiology, Xuanwu Hospital, Capital Medical University

Tel:861083199290

Email: yangyangqiqi@gmail.com

ABSTRACT

Background: Carotid artery intraplaque hemorrhage (IPH), an unstable component of atherosclerosis, is associated with an increased risk of stroke.

Purpose: To investigate quantitative susceptibility mapping (QSM) as a tool for the evaluation of IPH and calcification in vivo.

Study Type: Prospective

Population: Ten healthy volunteers and 15 patients

Field Strength/Sequence: 3.0 T Susceptibility-weighted imaging (SWI), magnetization-prepared rapid acquisition with gradient echo (MP-RAGE), T1-weighted Sampling Perfection with Application of optimized Contrasts using different flip angle Evolution (T1-SPACE), T2-weighted turbo spin-echo (T2WI) and time-of-flight (TOF) sequences.

Assessment: The vessel wall area of the carotid artery was measured on QSM and compared with T1-SPACE on healthy volunteers. The presence of IPH was determined on QSM and MP-RAGE by two reviewers separately and histology was used as a reference. The area of IPH was measured on QSM and MP-RAGE on matched slices. The area of calcification was measured on QSM and T1-SPACE on matched slices.

Statistical Tests: Bland-Altman analysis, Pearson correlation coefficients, linear regression analyses were performed to evaluate the concordance of area measurements. Cohen's kappa (κ) was analyzed to determine the agreement between IPH detections. Paired t-test was used to compare the group difference.

Results: In 423 matched slices, 20.1% (85/423) and 19.6% (83/423) were detected to have IPH on MP-RAGE and QSM, respectively. IPH detection by QSM and MP-RAGE showed good agreement ($\kappa = 0.822$, $P < 0.001$) between the two methods. There was no significant difference

in IPH area measurements between QSM and MP-RAGE ($7.28 \text{ mm}^2 \pm 6.41$ vs. $7.16 \text{ mm}^2 \pm 5.99$, $P = 0.575$). There was no significant difference in calcification area measurement between QSM and T1-SPACE ($3.51 \text{ mm}^2 \pm 1.78$ vs. $3.41 \text{ mm}^2 \pm 2.02$, $P = 0.783$).

Data Conclusion: QSM is a novel imaging tool for the identification of IPH in patients with carotid atherosclerosis and enables differentiation of IPH and calcification.

Key words: Carotid atherosclerosis; Quantitative susceptibility mapping; Intraplaque hemorrhage; Calcification

INTRODUCTION

Carotid atherosclerotic disease is a significant risk factor for ischemic stroke which is one of the leading causes of death and disability worldwide^[1-3]. Over the last decade, there has been greater emphasis on characterizing carotid plaque morphology and composition in addition to grading the degree of luminal stenosis^[4]. The key characteristics associated with increased stroke risks that have been identified on histopathologic specimens include: intraplaque hemorrhage (IPH), surface calcification, and the presence of a lipid-rich necrotic core^[5].

Currently, the assessment of carotid IPH is mainly based on magnetic resonance (MR) imaging techniques, such as time-of-flight (TOF), magnetization-prepared rapid acquisition with gradient echo (MP-RAGE) and T1-weighted Sampling Perfection with Application of optimized Contrasts using different flip angle Evolution (T1-SPACE) sequences. IPH signal intensity on MRI relies on erythrocyte integrity and the oxidation state of hemoglobin^[6]. Hemoglobin degrades from deoxyhemoglobin to methemoglobin in the acute status, and later to hemosiderin in the chronic stage. MP-RAGE has been demonstrated to have a high accuracy in carotid IPH detection validated by histology^[7]. However, a previous study showed that the sensitivity of MP-RAGE was decreased when detecting IPH with a small size or coexisting calcification^[8]. In addition, IPH progression or regression requires more quantitative MR imaging techniques to detect its small variations.

Quantitative susceptibility mapping (QSM) is a novel technique used to quantify tissue magnetic susceptibility properties^[9-11]. Recently, QSM has been proposed to differentiate diamagnetic calcifications and paramagnetic hemorrhages in the brain^[12] and a phase based method has been used for vessel wall imaging in the major peripheral arteries^[13]. Therefore, we proposed that it should also be able to detect and differentiate IPH and calcification in carotid atherosclerosis. Thus, the aim of this study was to develop a QSM protocol for the quantitative

evaluation of IPH and calcification *in vivo*.

MATERIALS AND METHODS

Study Population

This prospective study was conducted with institutional review board approval and all subjects signed the consent form. Ten healthy volunteers (mean age: 34.9 ± 11.4 years) were recruited. Fifteen patients (mean age: 66.3 ± 3.6 years) including ten patients scheduled for carotid artery stenting and five patients scheduled for carotid endarterectomy were prospectively included into the study. All 15 patients underwent carotid vessel wall imaging (VWI) and computed tomography (CT) angiography within one week. Inclusion criteria included patients who had symptomatic carotid artery stenosis of greater than 50% determined by Doppler ultrasound, CT or MR angiography. Three volunteers (mean age: 66.67 ± 3.33 years) who were suspected to have carotid artery stenosis were subsequently recruited for scan-rescan reproducibility analysis.

Carotid MR VWI Protocol

Subjects were imaged on a 3 Tesla scanner (Verio, Siemens Healthcare, Erlangen, Germany) with a dedicated eight-channel carotid coil. Fifteen patients underwent the carotid VWI protocol included: SWI, MP-RAGE, T1-SPACE, T2-weighted turbo spin-echo (T2WI), and TOF. Detailed imaging parameters are listed in Table 1. Three volunteers recruited for scan-rescan reproducibility analysis were scanned twice with proposed SWI acquisitions, with the two scans separated by 30 min off-table break when the subjects exited and reentered the scanner to be repositioned. These scans were referred to as Scan 1 and Scan 2.

QSM Imaging Protocol and Post-Processing Steps

The optimized QSM imaging protocol included three different susceptibility weighted imaging (SWI) acquisitions with echo times (TE) of 4.47 ms, 5.1 ms and 5.73 ms ^[9, 14]. Data from the TE

= 5.1 ms scan were used for the QSM reconstruction to eliminate the additional phase variation induced by the water/fat chemical shift as it was measured to be the in-phase time for fat surrounding the carotid vessel wall. Details are in the Supplementary Material.

For the data post-processing pipeline, we proposed 1) to keep only the phase information within the region of interest (e.g. carotid arteries, jugular veins and surrounding soft tissue) for a local QSM of the carotid artery to overcome the challenges including large field variation around the air/tissue interface (trachea) or bone closing to the carotid arteries and 2) to use a voxel-wise temporal domain approach to unwrap the original phase images^[14]. In the latter approach, the phase images from all three SWI acquisitions were used to unwrap the TE = 5.1 ms phase images which were subsequently used for QSM reconstruction. And the image post-processing pipeline is illustrated in Supplementary Material (Figure S3). The detailed QSM processing steps were as flows:

a) Image registration:

To prepare phase data for unwrapping, SWI data from TE = 4.47 ms and 5.73 ms were registered to data from TE = 5.1 ms in three steps: 1) separate left and right reference masks were generated for each subject semi-automatically by thresholding the 5.1 ms images to extract the carotid vessel region and dilating the resultant vessel mask to include adjacent soft tissues around each carotid region; 2) an affine registration using FLIRT was used^[15, 16]; and 3) a non-linear registration using FNIRT^[17, 18]. The detailed registration protocol is described in Supplementary Material.

b) Phase unwrapping:

A temporal domain phase unwrapping algorithm was applied to the co-registered data^[14]. Detailed steps are given in Supplementary Material.

c) Background field removal:

The unwrapped TE = 5.1 ms phase data was filtered using the sophisticated harmonic artifact reduction for phase (SHARP) data algorithm^[19] with a kernel size of 4 and deconvolution threshold of 0.05.

d) Dipole inversion:

The susceptibility maps were generated using a thresholded k-space division approach^[11].

Carotid VWI and QSM Image Analysis

T1-SPACE, MP-RAGE and QSM images were first registered and reformatted to cross-sectional slices with 2-mm slice thickness using a commercial software package (Vessel Analysis, Beijing, China). Four radiologists, blinded to clinical history and patient identity, then performed independent image analysis as follows: 1) outlining the lumen and wall boundaries on the three MR image sets, respectively; 2) determining the presence and area of IPH on MP-RAGE and QSM, respectively; 3) determining the area of calcification on T1-SPACE and QSM, respectively, by referring to CT image (thresholding at HU = 130^[20]) for the location. A time interval of at least 2 weeks between the interpretation of any two sequences by the same reader was used to avoid memory bias. All above quantitative measurements were averaged among the four readers and presence of IPH or calcification was finalized after consensus discussion.

Histopathology Analysis

Carotid endarterectomy specimens were excised intact without disruption of the luminal surface of the plaque. The specimen was fixed in 10% neutral buffered formalin, decalcified in 10% formic acid, and embedded en bloc in paraffin. Sections (10 μ m thick) were taken every 1.0 mm in the common carotid artery and every 0.5 mm in the internal carotid artery throughout the length of the specimen and stained with hematoxylin-eosin (H&E) and Mallory's trichrome stains. One pathologist first assessed all histopathologic specimens and selected regions of interest (ROIs) with

IPH blinded to clinical information. The histologic specimens were matched to the QSM images by used the landmarks such as the morphological features and the relative distance from the common carotid bifurcation. Then, two radiologists consensually drew ROIs on QSM images that matched the histologic sections

Scan-rescan Reproducibility Analysis

Scan-rescan reproducibility assessment was carried out for patients with two SWI scans, the area and mean susceptibility of the plaque were measured on the QSM data from both scans, Bland-Altman and linear regression analysis were performed to evaluate the reproducibility of proposed QSM method.

Statistical Analysis

Continuous values were expressed as mean \pm standard deviations, whereas categorical data were expressed as counts and percentages. Bland-Altman and linear regression analysis were performed to evaluate the concordance of vessel wall area measurements between QSM and T1-SPACE images in healthy volunteers. Cohen's kappa (κ) was analyzed to determine the agreement between QSM and carotid VWI data in identification of IPH and calcification. Bland-Altman analysis and Pearson correlation coefficients were evaluated to assess the correlations of IPH and calcification area between QSM and carotid VWI images. A paired t-test was used to compare the difference in IPH and calcification area between carotid VWI and QSM images. Agreement in IPH area measurement between QSM and histology was assessed using Spearman's correlation coefficient. A *P* value of less than 0.05 was considered as statistically significant. All statistical analyses were performed using SPSS version 22.0 (IBM, Armonk, NY, USA).

RESULTS

Patient Characteristics

Ten healthy volunteers and fifteen patients successfully underwent the proposed QSM and MR-VWI protocol. Eleven patients had unilateral and 4 patients had bilateral carotid atherosclerotic plaques.

Characterization of Vessel Wall and Plaque with QSM

Susceptibility maps from all subjects were successfully generated. The vessel wall area measurements on QSM and T1-SPACE images in healthy volunteers showed excellent correlation $R^2 = 0.826$ with a mean bias of $0.0065 \text{ mm}^2 \pm 0.019$ (Figure 1). IPH had positive susceptibility and appeared as a hyperintense region on QSM (Figure 2), whereas calcification had negative susceptibility and was depicted as a hypointense region (Figure 3). Figure 4 shows one typical case with complex plaque (co-existent IPH and calcification) which can be clearly depicted by QSM.

Comparison of IPH Detection between QSM and MP-RAGE

A total of 423 matched slices of the 15 patients scheduled for carotid artery stenting were included for analysis. From this group of slices, 20.1% (85/423) and 19.6% (83/423) were detected to have IPH on MPRAGE and QSM images, respectively. IPH detection by QSM and MP-RAGE showed good agreement ($\kappa = 0.822$, $P < 0.001$) (Table 2).

IPH Area Quantification on QSM and MPRAGE

There was no significant difference in IPH area measurement between QSM and MPRAGE ($7.28 \text{ mm}^2 \pm 6.41$ vs. $7.16 \text{ mm}^2 \pm 5.99$, $P = 0.575$, Figure 5a). Bland-Altman (Bias: $-0.12 \pm 2.17 \text{ mm}^2$, Figure 5b) and linear regression analysis ($R^2 = 0.886$; $P < 0.0001$, Figure 5c) showed good agreement between the two techniques for measuring the area of IPH.

Calcification Area Quantification on QSM and T1-SPACE

There was no significant difference in calcification area measurement between QSM and T1-SPACE ($3.51 \text{ mm}^2 \pm 1.78$ vs. $3.41 \text{ mm}^2 \pm 2.02$, $P = 0.783$, Figure 6a). Bland-Altman (Bias: -0.097

$\text{mm}^2 \pm 0.48$, Figure 6b) and linear regression analysis ($R^2 = 0.954$; $P < 0.0001$, Figure 6c) showed good agreement between the two techniques.

Ex-vivo Validation of IPH Detection on QSM

A total of 40 QSM slices were matched with histological sections from 5 patients who underwent carotid endarterectomy, of which 16 (40%) slices from 4 (80%) plaques had histology-detected IPH. IPH area measurements on QSM were correlated with histology (Spearman's $\rho = 0.78$, $P = 0.002$), an example of which is shown in Figure 7.

Scan-rescan Reproducibility Analysis

Both plaque area and mean susceptibility measurements showed good scan-rescan reproducibility. Bland-Altman (Bias: $0.119 \text{ mm}^2 \pm 0.623$) and linear regression analysis ($R^2 = 0.978$; $P = 0.001$) showed good agreement between the two scans for the area of the plaque. Bland-Altman (Bias: $0.022 \text{ ppm} \pm 0.101$) and linear regression analysis ($R^2 = 0.999$; $P < 0.0001$) showed good agreement between the two scans for measuring the mean susceptibility of the plaque.

DISCUSSION

In this study, we developed and evaluated a novel QSM protocol in the identification of carotid IPH and calcification in-vivo. QSM provided an accurate delineation of IPH and calcification when compared to other VWI methods (i.e., T1-SPACE and MP-RAGE).

Recently, a pilot study^[21] proved that QSM was capable of differentiate IPH, calcification and lipid rich necrosis. In our work, we proposed a local QSM approach by only keeping the region around the carotid arteries which removed outside regions that were not of interest but could lead to large-scale streaking artifact such as trachea (air-tissue interface), teeth (bone) and spinal cord (bone).

The signal intensity of IPH on MP-RAGE or other T1-weighted images depends on the acuity

of blood products. It is known that IPH experiences a dynamic degradation process, successively in the form of deoxyhemoglobin, methemoglobin, and hemosiderin^[23]. Among these blood products, methemoglobin is considered to be a source of high signal intensity because of its reduced T1. Therefore, MR signal may be complex due to the distribution and concentration of methemoglobin. A chronic inflammatory cascade incited by atherosclerosis can lead to a smaller apparent volume of IPH that over time leads to hemosiderin deposition or sequestration within foamy macrophages^[23]. This is supported by histologic findings of erythrocyte membranes and iron present within the necrotic cores of atherosclerotic coronary plaques even in the absence of recent hemorrhage^[24].

QSM is sensitive to the presence of blood degradation products. It will be able to differentiate blood from calcification at any stage of the hemorrhagic transformation process^[25]. Quantitative analysis of the mean susceptibility of vulnerable plaque may provide a meaningful measurement of the cumulative hemorrhagic plaque burden. The heterogeneity of clinical characteristics suggests the potential for subtle composition differences between symptomatic and asymptomatic IPH, which could be elucidated in future studies including QSM as part of VWI protocols.

QSM, due to its quantitative nature, may have the potential to determine the phase of atherosclerosis. According to the American Heart Association atherosclerosis classification criteria, certain phases are vulnerable to stroke and this variation in risk warrants close follow-up^[26]. On the other hand, QSM may help examine the effect of medical therapy on vulnerable plaque through quantitative analysis of the mean susceptibility of plaque content. Carotid QSM also paves the way for quantitative analysis of vulnerable plaque which is not feasible to the current VWI sequences.

Recently, a quantitative T1 mapping technique^[27] for vessel wall imaging has been proposed

to detect IPH. Compared to our proposed SWI protocol, quantitative T1 mapping is able to achieve higher and isotropic resolution with less scan time which could lead to more accurate measurements of curved vessel structures. However, QSM is sensitive to both hemorrhage and calcium, which makes it a potential tool for carotid plaque imaging of IPH and calcification simultaneously^[22]. QSM may also provide more quantitative information of IPH by overcoming the limitations of T1-weighted MR imaging. For example, IPH signal intensity on MRI is highly dependent on erythrocyte integrity and the oxidation state of hemoglobin. It degrades from methemoglobin in the acute stage to hemosiderin in the chronic stage, which can be detected on QSM images but is absent on MP-RAGE images.

Good scan-rescan reproducibility of both measured mean susceptibility values of the plaque and measured plaque area was observed in the three patients for the proposed QSM protocol. Although two separated scans were performed on the same subject for scan-rescan reproducibility analysis, the substantial change of subject's positioning after off-table break and the lack of established registration tools for human neck images dramatically increased the difficulty of accurate comparison between the two scans. Furthermore, we have only performed scan-rescan reproducibility analysis on three patients. Thus, a more comprehensive and robust study of interscan reproducibility of susceptibility mapping in the neck is of interest.

Our study has the following limitations. 1) To achieve three fully flow-compensated echoes, the current protocol requires three separate SWI acquisitions which prolongs the scan time. Future MR sequence development may enable collecting three fully flow-compensated echoes within one multi-echo SWI acquisition to dramatically reduce scan time. 2) The thresholded k-space division approach used for QSM reconstruction is a straightforward and efficient method to generate susceptibility maps, however, it may lead to systematic under-estimation of tissue susceptibility,

thus, more sophisticated methods could improve the accuracy of measured tissue susceptibility. 3) Although QSM is a quantitative MR technique, the correlation between the susceptibility and the amount of iron in the IPH has not been studied. 4) The through-plane resolution of QSM is lower than T1-weighted images. In this case, curved vessels have difficulty of being detected accurately compared to higher resolution imaging. 5) the patient population is small. Further investigation with a larger patient cohort may help define a threshold of susceptibility to identify IPH.

In conclusion, QSM may provide accurate carotid IPH detection and differentiation of blood products from calcification.

REFERENCES

1. Cohen SN, Hobson RW, 2nd, Weiss DG, Chimowitz M. Death associated with asymptomatic carotid artery stenosis: long-term clinical evaluation. VA Cooperative Study 167 Group. *J Vasc Surg*, 1993; 18: 1002-1011.
2. Gupta A, Baradaran H, Schweitzer AD, et al. Carotid plaque MRI and stroke risk: a systematic review and meta-analysis. *Stroke*, 2013; 44: 3071-7.
3. O'Leary DH, Polak JF, Kronmal RA, Manolio TA, Burke GL, Wolfson SK, Jr. Carotid-artery intima and media thickness as a risk factor for myocardial infarction and stroke in older adults. Cardiovascular Health Study Collaborative Research Group. *N Engl J Med*, 1999; 340: 14-22.
4. Kwee RM, van Oostenbrugge RJ, Prins MH, et al. Symptomatic patients with mild and moderate carotid stenosis: plaque features at MRI and association with cardiovascular risk factors and statin use. *Stroke*, 2010; 41: 1389-93.
5. Brinjikji W, Huston J, 3rd, Rabinstein AA, Kim GM, Lerman A, Lanzino G. Contemporary carotid imaging: from degree of stenosis to plaque vulnerability. *J Neurosurg*, 2016; 124: 27-42.
6. Gomori JM, Grossman RI, Yu-Ip C, Asakura T. NMR relaxation times of blood: dependence on field strength, oxidation state, and cell integrity. *J Comput Assist Tomogr*, 1987; 11: 684-90.
7. Crombag G, Schreuder F, van Hoof RHM, et al. Microvasculature and intraplaque hemorrhage in atherosclerotic carotid lesions: a cardiovascular magnetic resonance imaging study. *J Cardiovasc Magn Reson*, 2019; 21: 15.
8. Ota H, Yarnykh VL, Ferguson MS, et al. Carotid intraplaque hemorrhage imaging at 3.0-

- T MR imaging: comparison of the diagnostic performance of three T1-weighted sequences. *Radiology*, 2010; 254: 551-63.
9. Haacke EM, Liu S, Buch S, Zheng W, Wu D, Ye Y. Quantitative susceptibility mapping: current status and future directions. *Magn Reson Imaging*, 2015; 33: 1-25.
 10. Liu S, Wang C, Zhang X, et al. Quantification of liver iron concentration using the apparent susceptibility of hepatic vessels. *Quant Imaging Med Surg*, 2018; 8: 123-134.
 11. Haacke EM, Tang J, Neelavalli J, Cheng YC. Susceptibility mapping as a means to visualize veins and quantify oxygen saturation. *J Magn Reson Imaging*, 2010; 32: 663-76.
 12. Liu S, Buch S, Chen Y, et al. Susceptibility-weighted imaging: current status and future directions. *NMR Biomed*, 2017; 30.
 13. Yang Q, Liu J, Barnes SR, et al. Imaging the vessel wall in major peripheral arteries using susceptibility-weighted imaging. *J Magn Reson Imaging*, 2009; 30: 357-65.
 14. Feng W, Neelavalli J, Haacke EM. Catalytic multiecho phase unwrapping scheme (CAMPUS) in multiecho gradient echo imaging: removing phase wraps on a voxel-by-voxel basis. *Magn Reson Med*, 2013; 70: 117-26.
 15. Jenkinson M, Bannister P, Brady M, Smith S. Improved optimization for the robust and accurate linear registration and motion correction of brain images. *Neuroimage*, 2002; 17: 825-41.
 16. Jenkinson M, Smith S. A global optimisation method for robust affine registration of brain images. *Medical image analysis*, 2001; 5: 143-156.
 17. Jesper L. R. Andersson MJ, Stephen Smith. Non-linear registration, aka spatial normalisation. FMRIB technical report TR07JA2, 2010.
 18. Jenkinson M, Beckmann CF, Behrens TE, Woolrich MW, Smith SM. Fsl. *Neuroimage*,

- 2012; 62: 782-790.
19. Schweser F, Deistung A, Lehr BW, Reichenbach JR. Quantitative imaging of intrinsic magnetic tissue properties using MRI signal phase: an approach to in vivo brain iron metabolism? *Neuroimage*, 2011; 54: 2789-807.
 20. Saba L, Argiolas G, Siotto P, Piga M. Carotid artery plaque characterization using CT multienergy imaging. *American Journal of Neuroradiology*, 2013; 34: 855-859.
 21. Ikebe Y, Ishimaru H, Imai H, et al. Quantitative Susceptibility Mapping for Carotid Atherosclerotic Plaques: A Pilot Study. *Magnetic Resonance in Medical Sciences*, 2019.
 22. Manduteanu I, Simionescu M. Inflammation in atherosclerosis: a cause or a result of vascular disorders? *Journal of cellular and molecular medicine*, 2012; 16: 1978-1990.
 23. Azuma M, Maekawa K, Yamashita A, et al. Characterization of Carotid Plaque Components by Quantitative Susceptibility Mapping. *American Journal of Neuroradiology*, 2019.
 24. Wang Y, Spincemaille P, Liu Z, et al. Clinical quantitative susceptibility mapping (QSM): biometal imaging and its emerging roles in patient care. *Journal of Magnetic Resonance Imaging*, 2017; 46: 951-971.
 25. Arnett DK, Blumenthal RS, Albert MA, et al. 2019 ACC/AHA guideline on the primary prevention of cardiovascular disease. *Journal of the American College of Cardiology*, 2019; e596-e646.
 26. Qi H, Sun J, Qiao H, et al. Carotid intraplaque hemorrhage imaging with quantitative vessel wall T1 mapping: technical development and initial experience. *Radiology*, 2017; 287: 276-284.

TABLE**Table 1. MR imaging parameters for the proposed protocol.**

Scan	Orientation	TR (ms)	TE (ms)	FA (deg)	BW (Hz/px)	Resolution (mm ³)	Slices	Matrix Size	TA (min:sec)
SWI-1	Transversal	15	5.1	8	300	0.7×0.7× 2.0	64	256×256	3:07
SWI-2	Transversal	15	4.47	8	300	0.7×0.7× 2.0	64	256×256	3:07
SWI-3	Transversal	15	5.73	8	300	0.7×0.7× 2.0	64	256×256	3:07
MP- RAGE	Coronal	840	3.35	15	331	0.625×0.625 ×0.83	72	256×256	3:46
T1- SPACE	Coronal	800	24	120	514	0.625×0.625 ×0.63	64	256×256	5:46
TOF	Transversal	24	4.6	20	250	0.625×0.625 ×1	86	256×256	4:11

SWI, susceptibility-weighted imaging; MP-RAGE, magnetization-prepared rapid acquisition with gradient echo; T1-SPACE, T1-weighted Sampling Perfection with Application of optimized Contrasts using different flip angle Evolution; TOF, time-of-flight; TR, repetition time; TE, echo time; FA, flip angle; BW, bandwidth; TA: time to acquisition

Table 2. Agreement between QSM and MPRAGE imaging in identification of carotid IPH.

IPH detected by QSM imaging	IPH detected by MP-RAGE imaging		Cohen's kappa	<i>P</i> value
	Presence	Absence		
Presence	72	11	0.822	< 0.001
Absence	13	327		

IPH, intraplaque hemorrhage; QSM, quantitative susceptibility mapping

FIGURE LEGENDS

FIGURE 1. Consistency of the QSM and T1-SPACE data in measuring the vessel wall area on healthy volunteers as shown in a Bland-Altman plot (a) and a correlation of vessel wall area between T1-SPACE and QSM data ($R^2 = 0.826$, $P < 0.0001$) (b).

FIGURE 2. A 65-year-old male patient with right carotid atherosclerosis. MPRAGE image showing a hyperintense plaque component indicating IPH with an area of 17.13 mm^2 (red arrows indicate) (a). The IPH (yellow arrows) depicted on the SWI magnitude as a hypointense area (b). QSM demonstrated IPH as a hyperintense signal with an area of 15.48 mm^2 and a mean susceptibility value of 0.81 ppm compared to the adjacent arterial blood (green arrows), indicating a paramagnetic behavior and correlating well with MP-RAGE (c). Note that the vessel wall is diamagnetic and appears dark on susceptibility maps (with a mean susceptibility value of -0.21 ppm compared to the adjacent arterial blood) and also matches well with the vessel wall shown in the MP-RAGE image.

FIGURE 3. A hyperdense calcified component of a plaque depicted in the left carotid artery on a CT image (a). At the same position, SWI magnitude (b), MP-RAGE, where red arrow indicates flow artifacts (c), T1-SPACE (d) and QSM (e). Note that the susceptibility in the area of the calcification (blue arrows) is hypointense (with a mean susceptibility value of -0.89 ppm compared to the adjacent arterial blood) revealing a diamagnetic substance. The mean susceptibility value of the vessel wall is -0.28 ppm compared to the adjacent arterial blood.

FIGURE 4. A 66-year-old male patient with right carotid atherosclerosis. CT image showing two calcified plaques (indicated by the yellow arrows) in the right carotid artery (a). MP-RAGE image showing the right carotid artery with two calcified plaques (indicated by the yellow arrows) (b). The plaque components also included IPH shown as hyperintense (indicated by the red arrows)

and calcification shown as hypointense. The two sections indicated by the green arrows represent IPH and calcification that are hypointense in the SWI magnitude (c). QSM can distinguish the IPH (hyperintensity with a mean susceptibility value of 0.87 ppm compared to the adjacent arterial blood, indicated by red arrows) and calcification (hypointensity with a mean susceptibility value of -0.62 ppm compared to the adjacent arterial blood, indicated by yellow arrows) in the two sections (d). The mean susceptibility value of the vessel wall is -0.19 ppm compared to the adjacent arterial blood.

FIGURE 5. Comparison of the area of IPHs between QSM and MP-RAGE ($P = 0.575$) (a). Consistency between the MP-RAGE and QSM and data in measuring the IPH area (b). Correlation between MP-RAGE and QSM data in measuring the IPH area ($R^2 = 0.886$, $P < 0.0001$) (c).

FIGURE 6. Comparison of the area of calcification between QSM and T1-SPACE ($P = 0.783$) (a). Consistency between the T1-SPACE and QSM and data in measuring the calcification area (b). Correlation between T1-SPACE and QSM data in measuring the calcification area ($R^2 = 0.954$, $P < 0.0001$) (c).

FIGURE 7. Ex-vivo histology showing IPH (indicated by black circles) (a); Confirming the presence of intra-plaque hemorrhage on QSM (with a mean susceptibility value of 0.6 ppm compared to the adjacent arterial blood) (b).

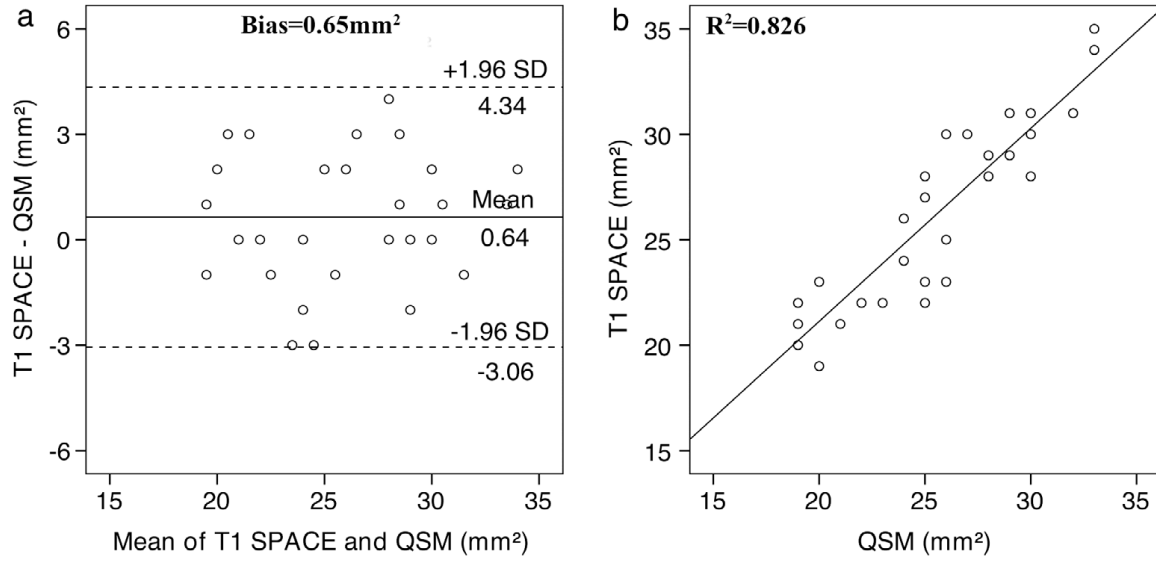


FIGURE 1. Consistency of the QSM and T1-SPACE data in measuring the vessel wall area on healthy volunteers as shown in a Bland-Altman plot (a) and a correlation of vessel wall area between T1-SPACE and QSM data ($R^2 = 0.826$; $P < 0.0001$) (b).

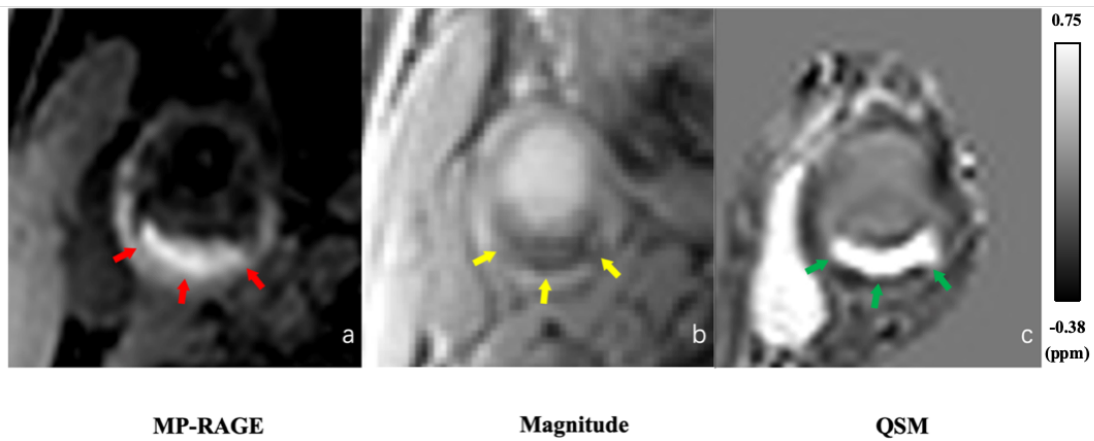


FIGURE 2. A 65-year-old male patient with right carotid atherosclerosis. MPRAGE image showing a hyperintense plaque component indicating IPH with an area of 17.13 mm^2 (red arrows) (a). The IPH (yellow arrows) depicted on the SWI magnitude as a hypointense area (b). QSM demonstrated IPH as a hyperintense signal with an area of 15.48 mm^2 and a mean susceptibility value of 0.81 ppm compared to the adjacent arterial blood (green arrows), indicating a paramagnetic behavior and correlating well with MP-RAGE (c). Note that the vessel wall is diamagnetic and appears dark on susceptibility maps (with a mean susceptibility value of -0.21 ppm compared to the adjacent arterial blood) and also matches well with the vessel wall shown in the MP-RAGE image.

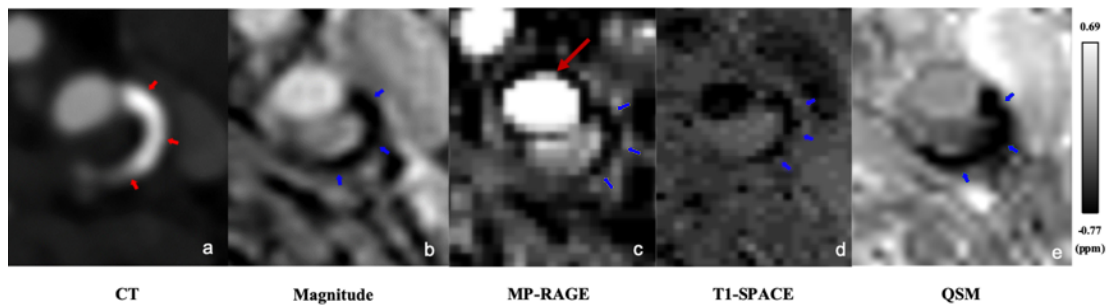


FIGURE 3. A hyperdense calcified component of a plaque depicted in the left carotid artery on a CT image (a). At the same position, SWI magnitude (b), MP-RAGE, where red arrow indicates flow artifacts (c), T1-SPACE (d) and QSM (e). Note that the susceptibility in the area of the calcification (blue arrows) is hypointense (with a mean susceptibility value of -0.89 ppm compared to the adjacent arterial blood) revealing a diamagnetic substance. The mean susceptibility value of the vessel wall is -0.28 ppm compared to the adjacent arterial blood.

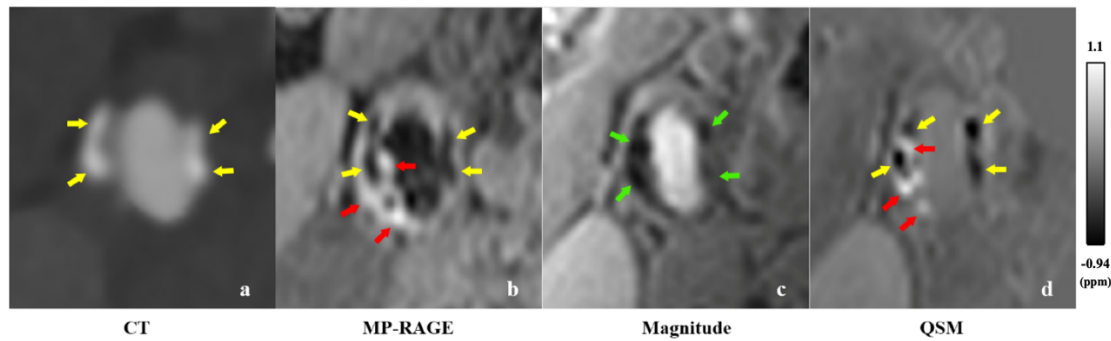


FIGURE 4. A 66-year-old male patient with right carotid atherosclerosis. CT image showing two calcified plaques (indicated by the yellow arrows) in the right carotid artery (a). MP-RAGE image showing the right carotid artery with two calcified plaques (indicated by the yellow arrows) (b). The plaque components also included IPH shown as hyperintense (indicated by the red arrows) and calcification shown as hypointense. The two sections indicated by the green arrows represent IPH and calcification that are hypointense in the SWI magnitude (c). QSM can distinguish the IPH (hyperintensity with a mean susceptibility value of 0.87 ppm compared to the adjacent arterial blood, indicated by red arrows) and calcification (hypointensity with a mean susceptibility value of -0.62 ppm compared to the adjacent arterial blood, indicated by yellow arrows) in the two sections (d). The mean susceptibility value of the vessel wall is -0.19 ppm compared to the adjacent arterial blood.

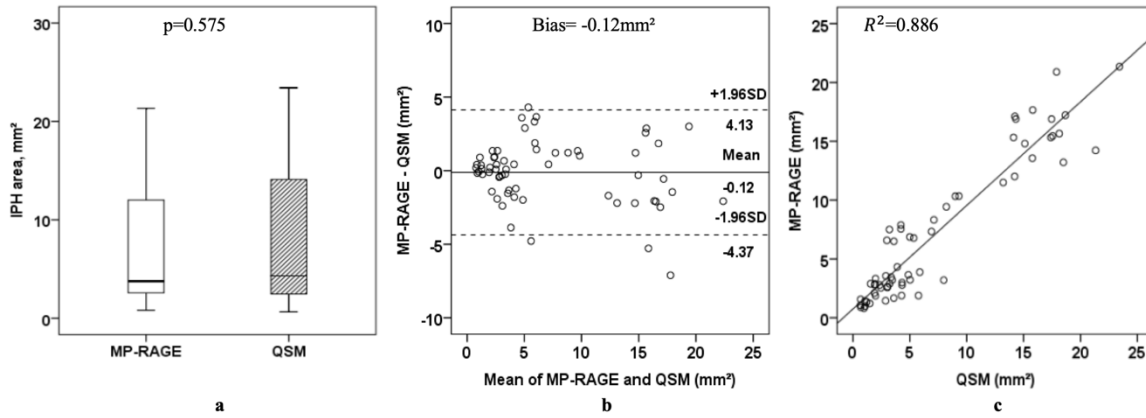


FIGURE 5. Comparison of the area of IPHs between QSM and MP-RAGE ($P = 0.575$) (a). Consistency between the MP-RAGE and QSM and data in measuring the IPH area (b). Correlation between MP-RAGE and QSM data in measuring the IPH area ($R^2 = 0.886$, $P < 0.0001$) (c).

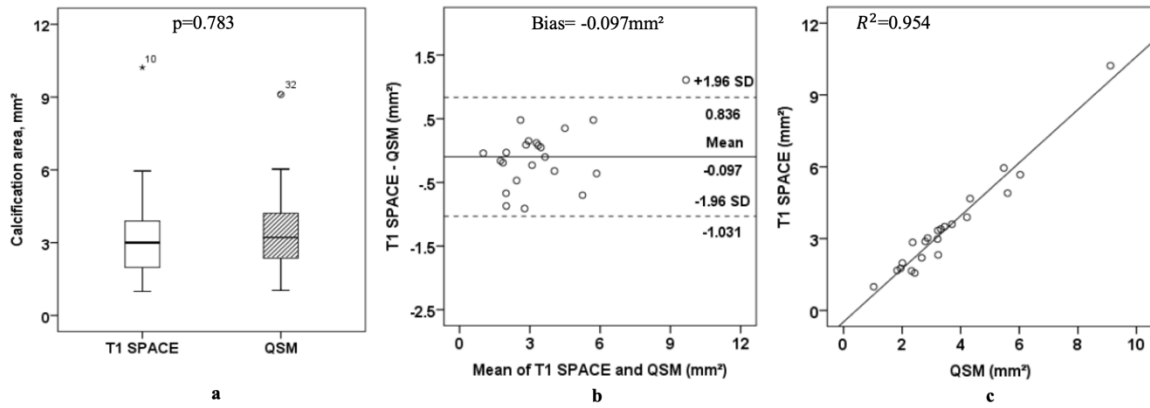


FIGURE 6. Comparison of the area of calcification between QSM and T1-SPACE ($P = 0.783$)

(a). Consistency between the T1-SPACE and QSM and data in measuring the calcification area

(b). Correlation between T1-SPACE and QSM data in measuring the calcification area ($R^2 = 0.954$,

$P < 0.0001$) (c).

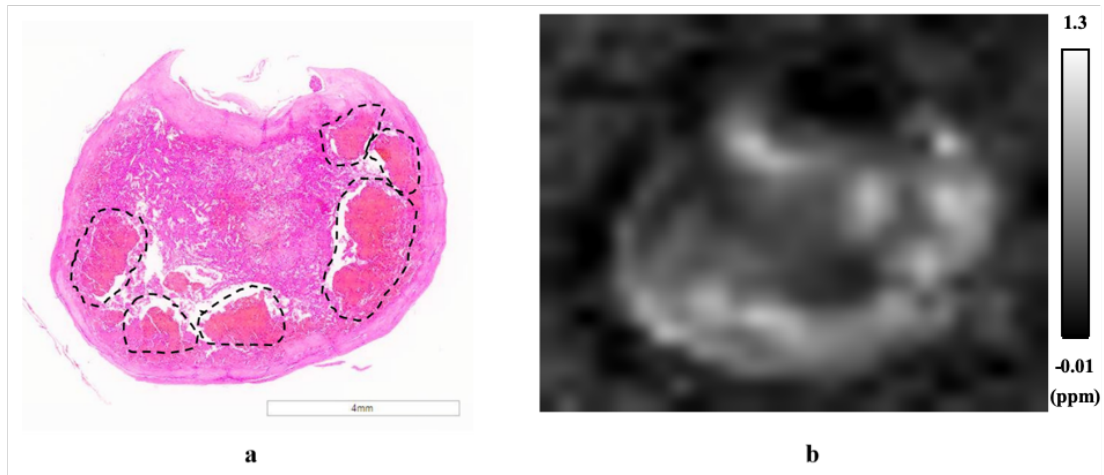


FIGURE 7. Ex-vivo histology showing IPH (indicated by black circles) (a); Confirming the presence of intra-plaque hemorrhage on QSM (with a mean susceptibility value of 0.6 ppm compared to the adjacent arterial blood) (b).

Acknowledgements

The authors thank Dr. Liquan Jiao (Department of Neurosurgery) and Dr. Yang Hua (Department of Ultrasonography) of Xuanwu Hospital, Capital Medical University, for providing pathological specimens.

Grant Support: This work was supported in part by the Beijing Natural Science Foundation (7191003), and the National Science Foundation of China (NSFC 81830056, 91749127).